The local atomic structure of di-alanine amino acid derivative of protoporphyrin IX

2007 J. Phys.: Condens. Matter 19 285214

(http://iopscience.iop.org/0953-8984/19/28/285214)

IOP PUBLISHING JOURNAL OF PHYSICS: CONDENSED MATTER

J. Phys.: Condens. Matter **19** (2007) 285214 (11pp) doi:10.1088/0953-8984/19/28/285214

The local atomic structure of di-alanine amino acid derivative of protoporphyrin IX

M S Walczak[1], K Lawniczak-Jablonska[1], A Sienkiewicz[1], M Czuba[2], M Klepka[1] and A Graczyk[2]

[1] Institute of Physics PAS, Aleja Lotnikow 32/46, 02-668 Warsaw, Poland
[2] Institute of Optoelectronics MUT, ulica Stefana Kaliskiego 2, 00-908 Warsaw, Poland

E-mail: mwalczak@ifpan.edu.pl

Received 15 October 2006, in final form 22 December 2006
Published 25 June 2007
Online at stacks.iop.org/JPhysCM/19/285214

Abstract

The photophysical and photochemical properties of photosensitizers bearing potential for photodynamic diagnosis (PDD) and treatment (PDT) of malignant tissues strictly depend on the details of their chemical processing. In this work, the x-ray absorption spectroscopy (XAFS) and electron spin resonance (ESR) techniques were applied to determine the nearest neighbourhood of iron in the di-alanine amino acid derivative of protoporphyrin IX (L-alanine diprotoporphyrinate). The investigated compound is a technological precursor for novel-class, highly water-soluble protoporphyrin IX-based photosensitizers, which have potential for applications in PDD and PDT and have just entered phase I clinical trials. Knowing the chemical content and exact atomic structures of the technological precursor, as well as of the high-purity final product, which all might contain some contamination, is a prerequisite for preparing photosensitizers for preliminary clinical tests.

1. Introduction

Photodynamic diagnosis (PDD) and photodynamic therapy (PDT) are novel medical modalities, which are increasingly being applied for the sensitive detection and treatment of malignant tissues. These methods combine the preferential accumulation of the photosensitizer in the target tissue with precise illumination, to provide the selectivity for cancer detection and treatment [1–8]. In PDT, light of an appropriate wavelength, adjusted to the chromophore absorption bands, penetrates the tissue and causes excitation of the photosensitizer. The excited photosensitizer reacts or transfers its energy to other molecules, thus generating cytotoxic species. It is widely accepted that the electronically excited form of molecular di-oxygen, singlet oxygen ($^1\Delta_g$), is a primary intermediate that is generated in the photodynamic treatment.

$^1\Delta_g$ is a highly reactive oxidizing agent that plays a significant role in a range of chemical and biological processes. Like other reactive oxygen species (ROS), singlet oxygen constitutes part of the extra/intracellular milieus of ROS that arise from cellular processes or are generated extracellularly. In the cellular milieu, high levels of $^1\Delta_g$ may give rise to a chain of chemical reactions, which ultimately lead to cell death. Although it is generally agreed that $^1\Delta_g$ is the major initiator of the photodynamic treatment, it is important to note that the role of other reactive oxygen species in PDT cannot be discounted [9]. It is well known that the iron-free derivative of heme (protoporphyrin IX) is a potent photosensitizing agent that acts via the formation of singlet oxygen [5, 9]. Although excellent photosensitizing properties of protoporphyrin IX were recognized early on and widely, its biomedical applications have often been restricted by the lack of readily available, non-expensive water-soluble derivatives. Recent breakthroughs, however, in derivatization, solubilization, and stabilization of water-soluble derivatives of protoporphyrin IX, generated a surge of interest in biological and medical applications of these compounds [10–13]. In this work, we report on structural features of the L-alanine-diprotoporphyrinate amino acid derivative of protoporphyrin IX, herein referred to as $PP(Ala)_2$. This compound is a technological precursor of another amino acid protoporphyrin IX-derivative, L-alanine, L-arginine-diprotoporphyrinate, herein referred to as $PP(Ala)_2(Arg)_2$. $PP(Ala)_2(Arg)_2$ is a newly developed water-soluble photosensitizer having a potential for applications in PDT. $PP(Ala)_2(Arg)_2$ acquires its excellent water-solubility due to the presence of two strongly hydrophilic arginine side-chains, which are connected to the central protoporphyrin-IX ring through carboxyl groups of propionic acids. The photophysical and photochemical properties of $PP(Ala)_2(Arg)_2$ are believed to be similar to those of parent photosensitizers containing iron-free protoporphyrin IX (e.g. Photofrin II) [9]. In particular, it has already been shown that $PP(Ala)_2(Arg)_2$ is a very good generator of singlet oxygen *in vitro* [14]. It has also been demonstrated that $PP(Ala)_2(Arg)_2$ reveals several other important features of a good photosensitizer for PDT applications, such as low intrinsic toxicity, excellent solubility in aqueous media and selective retention in malignant tissues. Moreover, in contrast to other currently used photosensitizers, $PP(Ala)_2(Arg)_2$ is readily cleared from the human body. Recent studies have shown that the characteristic quantum fluorescence and quantum yield of singlet oxygen generation in cell cultures are quite satisfactory [10, 11]. Thus, $PP(Ala)_2(Arg)_2$ seems to be a promising candidate for future clinical applications in PDT and recently entered Phase I clinical trials. It has to be stressed, however, that the technological processes of purification of the photosensitzer's substrates to the standard purity (a concentration of over 98%) are rather complicated and expensive. Therefore, current investigations of the photosensitizing properties of $PP(Ala)_2(Arg)_2$ on cellular lines, experimental animals and, most importantly, the clinical trials are based on mid-purity samples (of about 65%). Thus, the exact content and chemical structures of subsequent technological fractions and the final formula of the photosensitizer are now the subject of intensive studies. In particular, knowledge of the content and location of metal atoms impurities, including iron, will be especially useful for future modification and technology refining of this compound. This is of particular importance during the Phase I clinical tests, which target both necessary doses and side-effects, including toxicity. Hemin, which contains an iron atom inside the protoporphyrin IX ring, is the major substrate for obtaining $PP(Ala)_2$. Therefore, in this work, while using electron spin resonance (ESR) and extended x-ray absorption fine structure (EXAFS) techniques, we focused on the detection of iron atoms in $PP(Ala)_2$, which is a precursory fraction of the final photosensitizing product, $PP(Ala)_2(Arg)_2$. We also employed both these experimental techniques to investigate the nearest surroundings of the iron contaminants in $PP(Ala)_2$, the nominally iron-free technological precursor of $PP(Ala)_2(Arg)_2$.

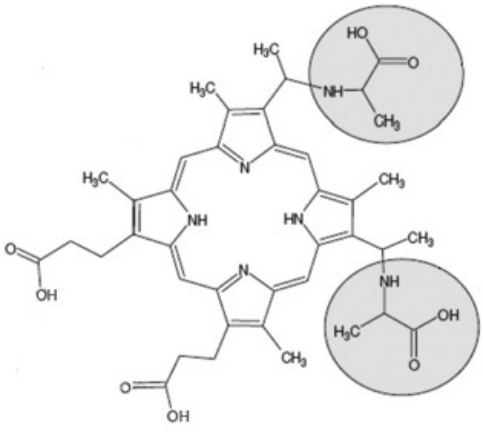

Figure 1. The postulated chemical structure of L-alanine diprotoporphyrinate, $PP(Ala)_2$. Two alanine (light grey) amino acids residues are attached to the iron-free protoporphyrin-IX ring.

2. Material

L-alanine-diprotoporphyrinate amino acid derivative of a protoporphyrin IX ($PP(Ala)_2$) sample was synthesized at the Department of Biochemistry and Spectroscopy, Institute of Optoelectronics, Military University Technology in Warsaw, Poland, following the technology described in [12, 13]. After synthesis, the obtained material was purified using standard column chromatography, which was then followed by high-performance liquid chromatography (HPLC). Subsequently, the solid phase was extracted using fractional elution technique, high thin-layer chromatography (HTLC), and HPLC methods. The purified sample of hemin was also investigated as a material of reference in this study. The postulated chemical structure of $PP(Ala)_2$ is depicted in figure 1. As can be seen in this figure, two side-chains of L-alanine (endogenous amino acid) are bound to the central protoporphyrin-IX ring via the vinyl bridges.

3. Experimental methods and data collection

The iron neighbourhood was examined using EXAFS and ESR techniques. EXAFS measurements using the transmission mode at the Fe–K absorption edge of the di-amino acid derivative of protoporphyrin IX and reference material, hemin, were performed at beamline BM26A at the European Synchrotron Radiation Facility. The energy scale was calibrated with reference to the metallic iron. The samples were cooled down to liquid helium temperature to reduce damage to the sample and temperature-induced disorder. A Si(111) two-crystal monochromator was used and higher harmonic reflections rejected by using the second mirror. The gas-ionization chambers were filled with an argon and helium mixture for transmission mode measurements. The data were collected in the 7090–8100 eV range, with a 0.5 eV near edge and a 2 eV further step. To achieve a reasonable signal-to-noise ratio, multiple scans were accumulated. EXAFS fine-structure isolation using a weighted cubic spline function and conversion to photoelectron wavevector k-space was performed with VIPER software [15]. The EXCURVE 9.275 program allowed further quantitative determination of the iron local atomic structure [16]. Standard field-swept ESR spectra of a $PP(Ala)_2$ sample were acquired using an X-band Bruker ESR spectrometer (Model ESP300E) at the Institute of Physics, Polish Academy of Sciences in Warsaw. Prior to performing ESR measurements, a powdered

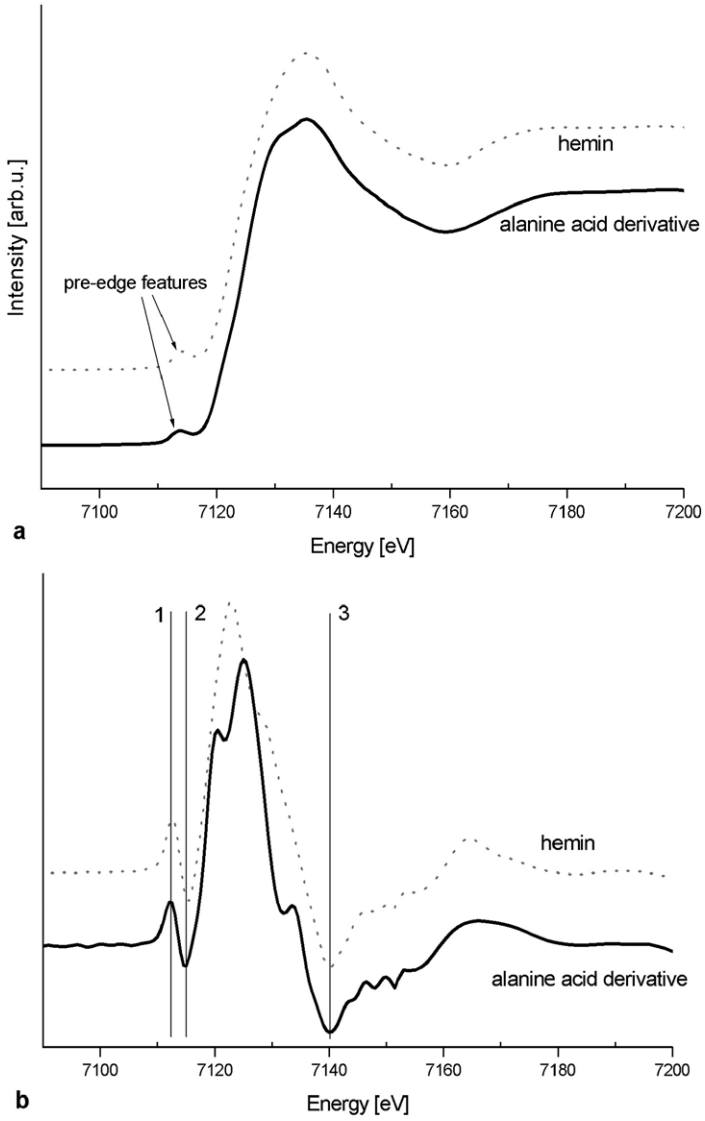

Figure 2. (a) X-ray absorption near iron K-edge spectra (XANES) of $PP(Ala)_2$ (solid line) and hemin (dotted line). (b) XANES first derivatives of $PP(Ala)_2$ (solid line) and hemin (dotted line). Vertical 1, 2, and 3 lines indicate the positions of characteristic features in the near-edge spectrum.

$PP(Ala)_2$ sample was suspended in ethylene glycol and transferred to a standard ESR quartz capillary having a 4 mm outside diameter (OD) and a 2.9 mm inside diameter (ID). Then, the sample was quenched at 77 K, transferred to the ESR cavity and rapidly cooled down to 4 K using an Oxford Instrument He gas flow cooling system.

4. Results and discussion

Despite thorough purification, the investigated sample of $PP(Ala)_2$ contained iron atoms, which was confirmed by both ESR and EXAFS. The XANES spectrum of $PP(Ala)_2$ is presented together with the reference spectrum of hemin in figure 2(a). The position of the XANES edge

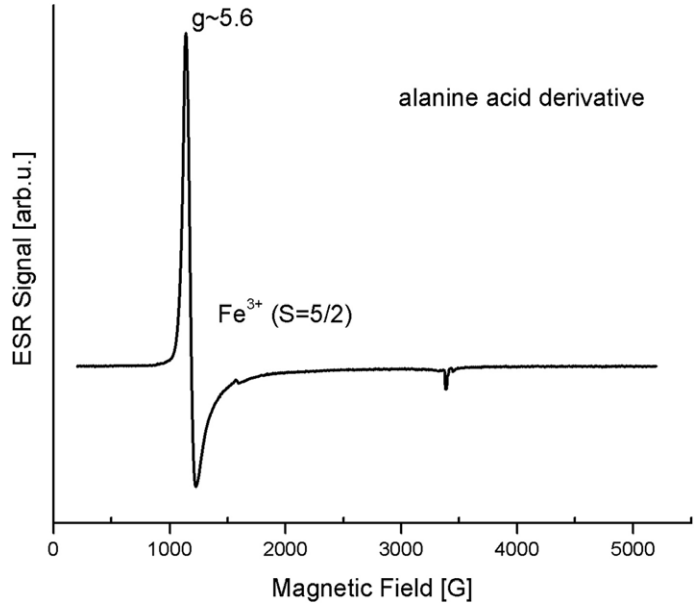

Figure 3. ESR spectrum acquired at 4 K for the frozen suspension of $PP(Ala)_2$ in ethylene glycol.

on the energy scale is strongly related to the ionic state of the absorbing iron atom. As can be seen in figure 2(b), which shows the first derivatives of the XANES spectra for both samples, these characteristic K-edge energies are the same for both compounds (within the margin of error of 0.5 eV).

In both cases the energy positions of the first maximum and second and third minimum are, respectively, 7112, 7115 and 7140 eV. It suggests that the iron ionic state in the investigated sample is close to that of hemin, which is considered to be trivalent (3+) [17]. Additional evidence for this is the presence of a characteristic Fe^{3+} pre-edge feature in XANES (indicated by arrows in figure 2(a)). The similarity of XANES shapes over the whole energy range suggests that iron in $PP(Ala)_2$ has a similar atomic surrounding as in hemin. Nevertheless, a slight difference in the left slope of the absorption edge indicates that this surrounding is not entirely identical [18]. Chlorine is the atom nearest to the iron atom in the hemin structure and chlorine is positioned outside the heme plane. The differences in the XANES spectra of $PP(Ala)_2$ and hemin between 7120 and 7135 eV then suggest another chlorine ligand in the di-alanine derivative. This conclusion is in concurrence with the ESR results. The g-factor and shape of the ESR spectrum (figure 3) can be interpreted as originating from high-spin ($S = 5/2$) trivalent iron (Fe^{3+}), described by a nearly axial spin Hamiltonian. This points to an axial local symmetry of the iron atoms in the investigated compound.

The ESR spectrum also indicates that trivalent iron occurs in significant amounts only at one site in the $PP(Ala)_2$ molecule, which seemed to be the centre of the protoporphyrin IX ring, taking into consideration what is determined by the ESR symmetry of the iron. The conclusions from the XANES and ESR spectra search give us the starting structure model to be used in quantitative EXAFS analysis, i.e. the crystallographic resolved structure of hemin containing a protoporphyrin IX plane with a trivalent high-spin iron centre. The preparation of spectra for further analysis was as follows. The raw fine-structure EXAFS oscillations of both investigated and reference compounds without noise removal or Fourier filtering were multiplied to the third power of the internal photoelectron wavevector and limited to the 3.2–16 $Å^{-1}$ range (figure 4).

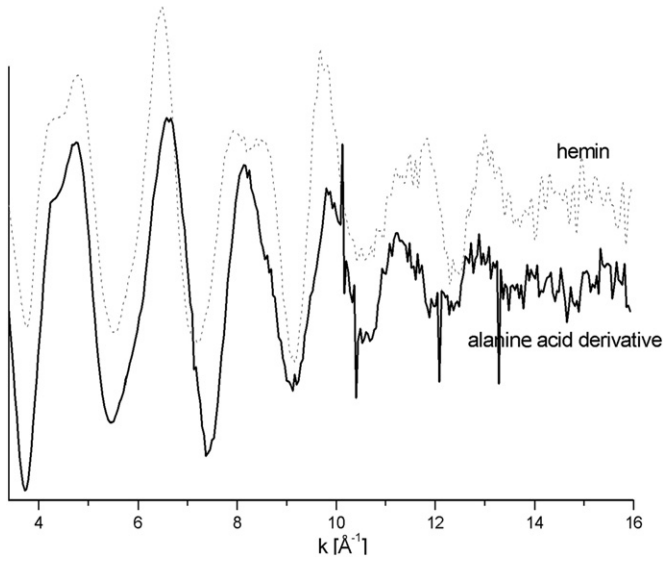

Figure 4. EXAFS oscillation function of $PP(Ala)_2$ and reference compound, hemin.

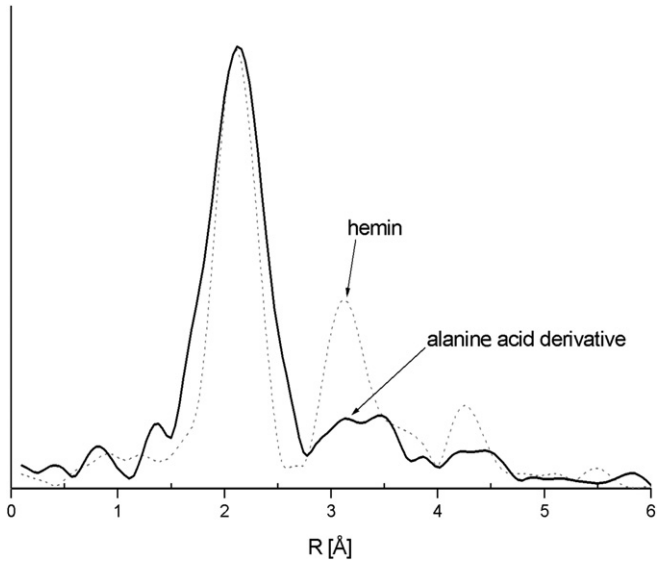

Figure 5. EXAFS Fourier transform function of $PP(Ala)_2$ and reference compound, hemin.

Examining the shape of the EXAFS oscillations' Fourier transform (figure 5), one can notice that the first shell has a wider amplitude then hemin. This strongly suggests the presence of an atom heavier than chlorine as a non-heme plane ligand. The contribution of further carbon atoms, which appear in the second peak located at around 3.5 Å, is much stronger in hemin. After examining the process of synthesis of $PP(Ala)_2$, the suspicion arises that a bromine atom may be one of the nearest neighbours of iron. Therefore, a model replacing chlorine with a bromine atom and adjusting the Fe–Br distance to 2.4 Å was considered. The summation of

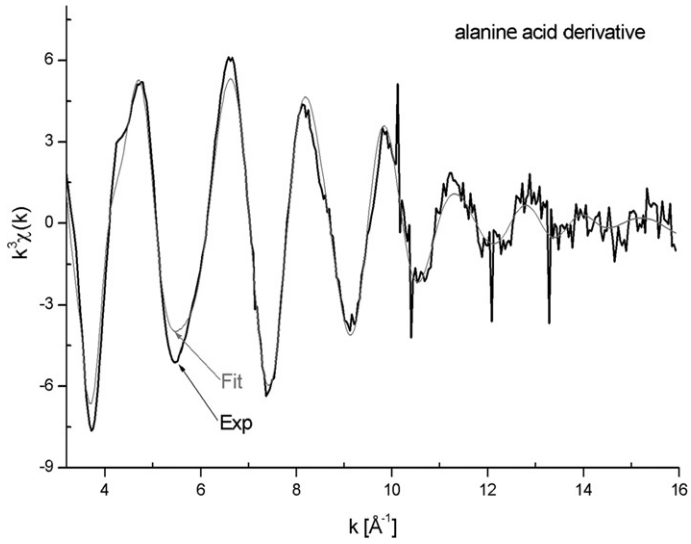

Figure 6. EXAFS oscillation function of $PP(Ala)_2$ (black line) and theoretical calculated spectra (grey line) using refining parameters. Accord with experiment is given by an *R*-factor equal to 23.15.

the elementary contribution to the EXAFS oscillation function of the atoms nearest to iron was performed using a theoretical phase-shift and amplitude scattering function calculated using the EXCURVE 9.275 program. To perform a refining procedure, the iron's surroundings was limited to a spherical radius of 4.34 Å. The addition of atoms at further distances did not improve the fitting due to the quality of the experimental data and the high level of noise. The refining procedure was performed in accordance with the receipt given in [19]. Assuming the crystallography structure of the heme group and substituting a bromine iron ligand instead of a chlorine iron ligand, the fitting procedure for a $PP(Ala)_2$ EXAFS function could be performed simultaneously within the whole region being examined. The strategy for the fitting procedure was as follows. The atoms in the molecule being considered were divided into five shells. The shells, counting from the nearest to iron, contained, respectively, four nitrogen atoms, one bromine atom, eight carbon atoms, four carbon atoms and eight carbons. Due to the many fitting parameters, at first a constrained refinement was performed. Values of the Debye–Waller factor were kept equal for atoms belonging to the same shell, and the distances between atoms inside a particular shell did not change, but all the atoms were moving simultaneously with respect to the absorber. Multi-scattering paths were also considered and the amplitude-damping factor S_o was set to be equal to one. Next, restrained refinement was performed and, during fitting, the distances from the central iron for each atom in the shell were adjusted separately, while the Debye–Waller factors remained the same for atoms at similar distances from the iron and similar surroundings. The errors of the refining parameters were automatically calculated using the Excurve 9.275 program during the fitting procedure. The resulting fit of the EXAFS function is presented in figure 6. Fitting parameters are collected in tables 1 and 2. Figure 7 shows the Fourier transform of the experimental and calculated EXAFS.

The same above-described fitting procedure was applied to refine the hemin structure, but this time crystallographic positions and the kind of atoms were not modified before starting, and the second shell was a chlorine atom. The refinement of the EXAFS hemin oscillations and its Fourier transform, together with the respective row spectra, are presented in figures 8

Table 1. Iron–atom distance parameters for hemin crystallography resolved and hemin and $PP(Ala)_2$ EXAFS oscillation function refining. The fitting error were estimated to be below 0.005 Å.

	Distances from Fe (Å)		
Atoms	Hemin crystallography	Hemin EXAFS	$PP(Ala)_2$ EXAFS
N	2.046	2.054	1.945
N	2.057	2.057	2.031
N	2.066	2.067	2.064
N	2.081	2.073	2.109
Cl\Br	2.220	2.223	2.36
C	3.061	3.069	2.990
C	3.073	3.076	3.005
C	3.081	3.078	3.034
C	3.083	3.091	3.099
C	3.100	3.092	3.118
C	3.103	3.105	3.119
C	3.112	3.106	3.131
C	3.116	3.113	3.141
C	3.446	3.443	3.322
C	3.449	3.451	3.372
C	3.466	3.461	3.405
C	3.467	3.472	3.422
C	4.284	4.287	4.158
C	4.286	4.291	4.230
C	4.292	4.292	4.249
C	4.299	4.298	4.273
C	4.315	4.323	4.275
C	4.334	4.327	4.340
C	4.339	4.341	4.377
C	4.358	4.350	4.439

Table 2. Debye–Waller factors of hemin and $PP(Ala)_2$ EXAFS oscillation function refining.

	Debye–Waller factors $2\sigma^2$ (Å^2)	
Atoms	Hemin EXAFS	PP(Ala)2 EXAFS
Shell 1 4 N	0.008 ± 0.010	0.003 ± 0.0008
Shell 2 Cl\Br	0.005 ± 0.004	0.012 ± 0.008
Shell 3 8 C	0.006 ± 0.003	0.054 ± 0.042
Shell 4 4 C	0.009 ± 0.006	0.009 ± 0.002
Shell 5 8 C	0.016 ± 0.004	0.022 ± 0.008

and 9. The refining parameters are collected in table 1, together with the parameters for the investigated protoporphyrin IX in table 2.

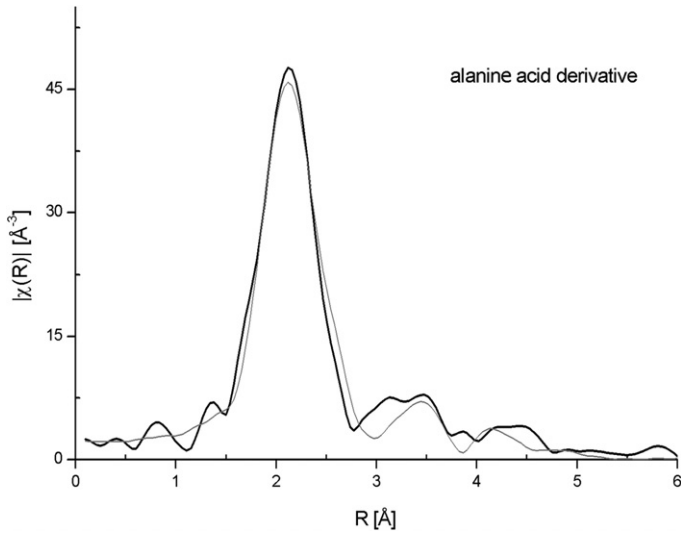

Figure 7. Fourier transform of experiment (black line) and theoretical calculated EXAFS (grey line) functions for $PP(Ala)_2$.

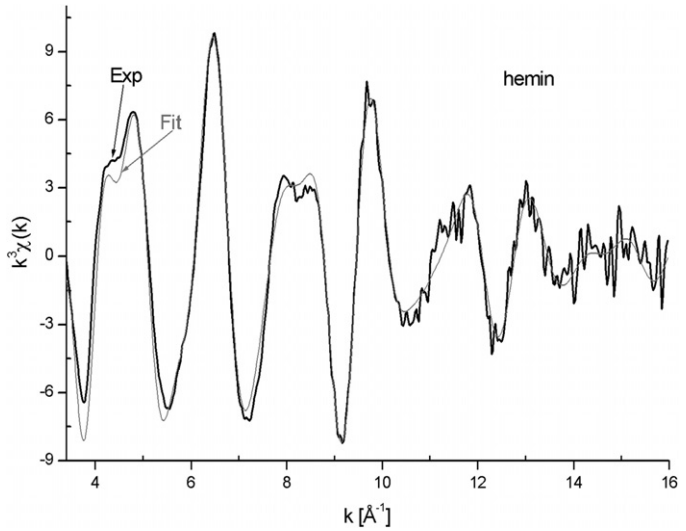

Figure 8. EXAFS oscillation function of hemin (black line) and theoretical calculated spectra (grey line) using refining parameters. Accord with experiment is given by an *R*-factor equal to 19.72.

The analysis of $PP(Ala)_2$ provided the distances from the iron to each atom in a particular shell. The values of the distances of the atoms, ascribed to the same shell, do not differ significantly. This proved that the symmetry of the heme plane is preserved around iron atoms in the sample investigated. However, this plane is more distorted then in hemin (see table 1). The differences in distance from iron for the closest and most outlying atoms inside the given shell in hemin are 0.019 Å (first shell) and 0.044 Å (third shell). The same differences for $PP(Ala)_2$ for the first and third shells are, respectively, 0.064 and 0.142 Å. Reasonable Debye–Waller factors for nitrogen, bromine and 12 peripheral carbon atoms for the di-alanine

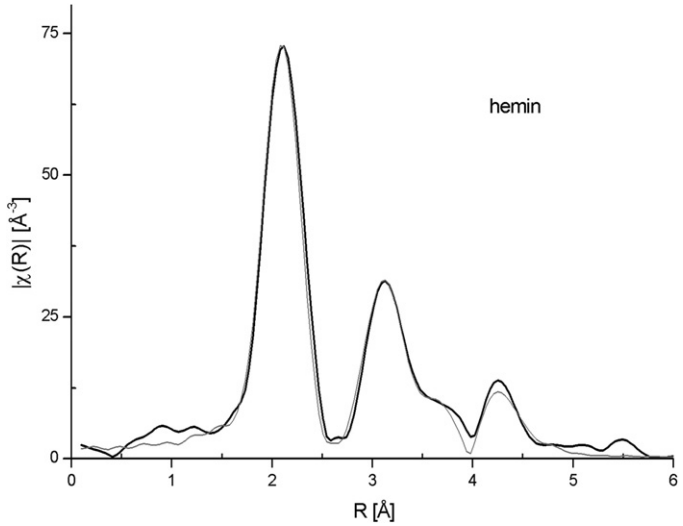

Figure 9. Fourier transform of experiment (black line) and theoretical calculated EXAFS (grey line) functions for hemin.

derivative were achieved (see table 2). The *R*-factor value of 23.15 indicates good agreement with experiment. Worrisome is the quite high (0.054) Debye–Waller factor for the third shell of carbons. There is no possibility of explaining this by temperature disorder. The sample was cooled down to a few Kelvin. Considering the above, it is highly probable that there is some chemical disorder in protoporphyrin IX, or there are some additional light atoms attached outside the heme plane inside the analysed radius from the iron centre (i.e. at an average distance of 3 Å). It can also be an explanation for the distortion found inside the heme ring. This requires further experiments and analysis of the local atomic structure around the bromine atoms from studies of the K-absorption edge of bromine.

5. Conclusion

The successfully performed EXAFS analysis of the Fe K-edge measured for the di-alanine acid derivative of protoporphyrin IX allowed us to determine the local environment of the iron atoms in this compound. The presence of bromine, the additional heavy metal, was detected and a plausible location for this atom was proposed. The analysis of bromine x-ray absorption fine structure will help in a more detailed determination of the local atomic structure around this atom. The structural information concerning the nearest neighbourhood of iron in $PP(Ala)_2$ is of great importance. It may help to improve the efficiency of subsequent technological steps for obtaining $PP(Ala)_2$ (purification processes), as well as evaluating the influence of iron contaminants on the quantum fluorescence yield and quantum efficiency for singlet oxygen generation for mid-purity compounds. The analysis that has been presented also confirms the usefulness of the EXAFS technique for the investigation of biological noncrystalline materials.

Acknowledgments

We acknowledge the European Synchrotron Radiation Facility for the provision of synchrotron radiation facilities, and we would like to thank Sergey Nikitenko for assistance in using the beamline BM26A.

References

[1] Miller J 1999 *J. Chem. Educ.* **76** 592
[2] Dolmans D E J G J, Fukumura D and Jain R K 2003 *Nat. Rev. Cancer* **3** 380
[3] Wilson B C 2002 *Can. J. Gastroenterol.* **16** 393
[4] Vrouenraets M B, Visser G W M, Snow G B and van Dongen G A M S 2003 *Anticancer Res.* **23** 505
[5] Dougherty T J *et al* 1998 *J. Natl Cancer Inst.* **90** 889
[6] Dickson E F G, Goyan R L and Pottier R H 2003 *Cell. Mol. Biol.* **48** 939
[7] Capella M A M and Capella L S 2003 *J. Biomed. Sci.* **10** 361
[8] 2003 http://www.accessdata.fda.gov/scripts/cder/onctools/linelist.cfm?line=Palliative
[9] DeRosa M C and Crutchley R J 2002 *Coord. Chem. Rev.* **233/234** 351
[10] Ye S, Czuba M, Romiszewska A, Karolczak J and Graczyk A 2003 *Opt. Appl.* **33** 489
[11] Ye S, Kwasny M, Czuba M and Graczyk A 2003 *Opt. Appl.* **33** 505
[12] Graczyk A and Konarski J 1995 *US Patent Specification* No 005451599A
Graczyk A and Konarski J 1997 *European Patent Specification* No 0539960A2/97
[13] Konarski J 1990 *PL Patent Specification* No 148775 (in Polish)
[14] Vileno B, Sienkiewicz A, Lekka M, Kulik A J and Forro L 2004 *Carbon* **42** 1195
[15] Klementiev K V 2001 *J. Phys. D: Appl. Phys.* **34** 209 VIPER for Windows, freeware: www.desy.de/~klmn/viper.html
[16] Gurman S J, Binsted N and Ross I 1986 *J. Phys. C: Solid State Phys.* **19** 1845
[17] Tsutsui K 1986 *Methods Enzymol.* **123** 331
[18] Pin S, Valat P, Cortes R, Michalowicz A and Alpert B 1985 *Biophys. J.* **48** 997
[19] Strange R W and Hasnain S 2005 *Methods Mol. Biol.* **305** 167